Journal Name

COMMUNICATION

SERS Enhancement of Silver Nanoparticles Prepared by a Template-Directed Triazole Ligand Strategy

Received 00th January 20xx,
Accepted 00th January 20xx

DOI: 10.1039/x0xx00000x

www.rsc.org/

Heba A. Kashmery,[a] David G. Thompson,[b] Ruggero Dondi,[c] Samuel Mabbott,[b] Duncan Graham,[b] Alasdair W. Clark,[d] Glenn A. Burley[a]**

Two advances in the development of a one-pot method to prepare silver nanoparticles (AgNPs) using the Tollens' reagent are described. First, a template-directed process of AgNP synthesis using resorcinol triazole ligands bearing two pendent galactose sugars is shown. Second, the conversion of these AgNPs into SERS nanotags is demonstrated using malachite green isothiocyanate as the Raman reporter molecule.

This manuscript reports a new method to form silver nanoparticles (AgNPs) using sugar triazole ligands bearing short ethyleneglycol (EG) chains. By virtue of their enhanced optical absorption relative to gold nanoparticles (AuNPs), AgNPs hold considerable potential as highly sensitive biodiagnostic and imaging platforms,[1] yet a key challenge that needs to be addressed is access to facile, mild and reliable preparative methods where the parameters of size, shape and surface coating are inherently controllable, and indeed reproducible.[2] The most common methods used to prepare AgNPs involve the reduction of silver salts using sodium borohydride,[3] or citrate[4] as the corresponding reducing agents, producing AgNPs of varying degrees of dispersity and shape control.[1b] The polyol method[5] of AgNP synthesis enhances both size and shape control, but requires careful stoichiometric control of reagents and additives at 140-160 °C.[6] Seeded growth methods provide an alternative to the polyol method of synthesis of AgNPs, although extra synthetic steps are required, which increases the complexity of this approach.[7]

The utilization of reducing sugars in the presence of the Tollens' reagent [Ag(NH_3)]OH provides a mild and facile strategy forming stable AgNP colloids in a single step without the need of specialised equipment.[8] We have recently reported a template-directed variant of the Tollens' reaction that forms monodispersed AgNPs where the parameters of nanoparticle size, shape and colloidal stability are tightly controlled by the use of triazole ligands (*e.g.,* **1-2**).[9] These molecules putatively perform multiple functions. Firstly, the triazole core binds Ag(I), bringing this cation within close proximity to the corresponding galactose reducing sugars. The pendent sugars reduce Ag(I) to Ag(0) and facilitate the growth of Ag(0) clusters into AgNPs. Finally, the overall scaffold passivates the AgNP surface to produce stable suspensions in aqueous buffers.[9b] We have previously shown that the lower affinity ligand (**2**) produces monodisperse AgNPs where the size (*i.e.,* 16 ± 3 to 30 ± 4 nm) and shape is tuneable according to the reaction conditions.

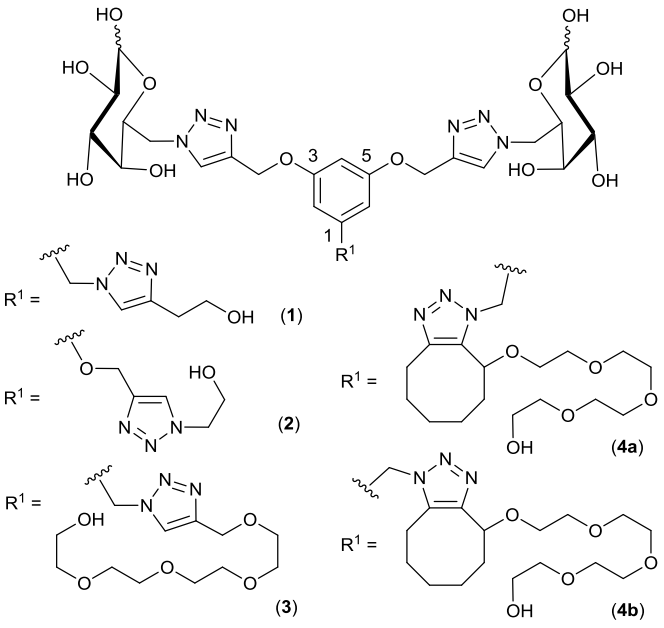

Fig. 1. Structures of sugar triazole ligands (**1-4**).

[a] *WestCHEM & Department of Pure & Applied Chemistry, University of Strathclyde, 295 Cathedral Street, Glasgow, G1 1XL, UK. Email: glenn.burley@strath.ac.uk*
[b] *Centre for Molecular Nanometrology, Department of Pure & Applied Chemistry, University of Strathclyde, 295 Cathedral Street, Glasgow, G1 1XL, UK. Email: duncan.graham@strath.ac.uk*
[c] *University of Bath, Department of Pharmacy and Pharmacology, Claverton Down, Bath, BA2 7AY, UK.*
[d] *Biomedical Engineering Research Division, School of Engineering, Rankine Building, Oakfield Avenue, University of Glasgow, Glasgow, UK. Email: alasdair.clark@glasgow.ac.uk*

Electronic Supplementary Information (ESI) available: Experimental procedures and characterisation data.

In contrast, ligand (**1**) displayed a significantly higher Ag(I)-binding affinity, resulting in the formation of AgNPs 8 ± 5 nm in diameter over a wide concentration range of both ligand and Tollens' reagent.

In order to enhance the modularity of AgNP synthesis for biosensing applications, a synthetic platform is required that enables facile access to the central Ag-binding core and the ability to detect analytical changes within an aqueous environment. Hydrophilic tethers such as polyethyleneglycol chains are used extensively in nanoparticle bioconjugates to enhance nanoparticle solubility and stability;[1e] however their effect on the template-directed formation of AgNPs has not been explored. A modular route to explore the impact of these tethers on AgNP synthesis and biosensing capability would involve their installation in the southernmost portion of the ligand using bio-orthogonal Cu(I)-catalysed and copper-free click chemistry.[10,11]

We describe herein the preparation of size and shape-selected AgNPs templated by ligands (**3**, **4a-b**) bearing EG tails. Furthermore, we show the conversion of these AgNPs into SERS nanotags by the conjugation of malachite green isothiocyanate (MGITC) to the AgNP surface. SERS nanotags have been used extensively in several high profile studies including *in vivo* imaging by SERS with MGITC one of the preferred Raman reporters within the nanotag.[1d, 12] The synthetic approach offered by the triazole ligands allows easy preparation of the nanotags as demonstrated initially by using the MGITC.

The structural impact of the southernmost triazole on the preparation of AgNPs was explored by two approaches. The first involved a Cu(I)-catalysed [3+2] cycloaddition between azide (**5**) and alkyne (**6**), followed by acid-mediated deprotection of the isopropylidene groups to produce (**3**) in 40% yield (Scheme 1).

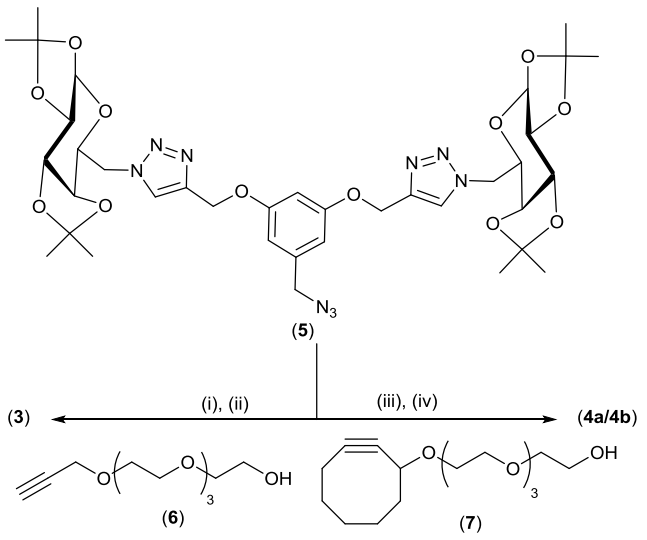

Scheme 1. *Reagents and conditions:* (i) (**6**) (6.0 equiv.), $CuSO_4$ (0.1 M, 1.2 equiv.), sodium ascorbate (2.0 equiv.), THF: H_2O (3:1), 70%; (ii) TFA: H_2O (1:1), reflux, 70°C, 4h, 40%; (iii) (**7**) (1.8 equiv.), DMSO, rt, 24h, 37% : 26% (**4a : 4b**); (iv) TFA: H_2O (1:1), reflux, 70°C, 3h, 77 %.

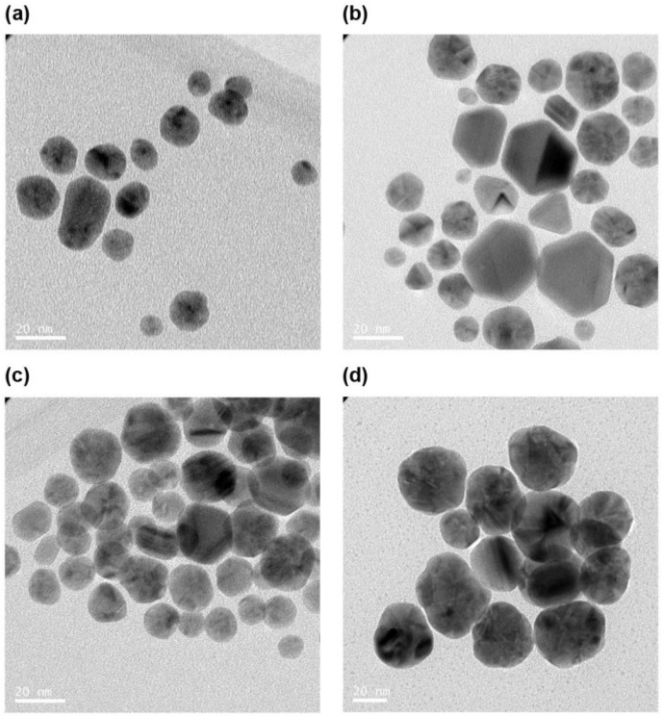

Fig. 2. Exemplar TEM images of **(a)** AgNP@(**3**) using 10 mM Tollens' and 10 mM (**3**), Ø = 15 ± 4 nm. **(b)** AgNP@(**4a**) using 10 mM Tollens' and 10 mM (**4a**), Ø = 18 ± 7 nm. (**c**) AgNP@(**4b**) using 10 mM Tollens' and 10 mM (**4b**), Ø = 17 ± 5 nm. (**d**) 10 mM Tollens' and 25 mM (**4b**), Ø = 38 ± 7 nm.

The second approach involved installing a southernmost triazole via a copper-free [3+2] cycloaddition between (**5**) and (**7**).[10a] This reaction formed two regioisomers in a 1.4:1.0 ratio (total yield 63%). Acid deprotection of the isopropylidene groups afforded pure (**4a**) and (**4b**) after RP-HPLC. The formation of AgNPs was then screened as a function of [ligand] and [Tollens'].[9] Angular AgNP@(**3**) of similar sizes [15 ± 4 nm] were formed over a wide concentration range (Fig. 2a, Fig. S4a, Table S1), whereas the formation of AgNP@(**4a**) required a much narrower concentration window (Table S2). TEM analysis of several examples in this series produced angular AgNP@(**4a**) with diameters ~18 ± 7 nm (Fig. 2b, Fig. S4c-d). The formation of AgNPs was then investigated using ligand (**4b**). Consistent with the formation of AgNP@(**4a**), a similar concentration window for their formation was observed (Table S3), although the sizes of angular AgNP@(**4b**) formed were inherently tunable according to the reaction conditions. For example, TEM analysis revealed sizes AgNP@(**4b**) of diameters ranging from 17 ± 5 nm (Fig. 2c) to 38 ± 7 nm nm (Fig. 2d). We therefore conclude that the regiochemistry of the southernmost triazole in ligands (**4a**) and (**4b**) significantly influences the size of AgNPs formed.

The kinetics of AgNP formation was then explored using **3, 4a-b** by monitoring the onset of the surface plasmon peak at 400 nm using 20 mM [ligand] and 20 mM [Tollens']. Both the onset (~200 s) and end-point (~1000 s) of the formation of AgNP@(**4a**) were significantly faster than AgNP@(**3**) [onset ~ 900 s; end-point ~2000 s], whereas the kinetics of AgNP@(**4b**) [onset ~ 1100 s; end-point ~ 2900 s] was significantly slower than both AgNP@(**3**) and AgNP@(**4a**) (Fig. S5).

^{1}H NMR titration experiments using $AgNO_3$ were conducted to determine the Ag(I) binding affinities of each ligand.[13] A 0.10 ppm downfield shift of triazole (H^a) and a 0.08 ppm upfield shift (H^b) was observed upon the addition of three equivalents of Ag(I) to compound (**3**) (Fig. S6). The addition of a further three equivalents of Ag(I) resulted in a continual downfield (0.13 ppm) and upfield (0.09 ppm) shifts of H^a and H^b respectively. Although the downfield shift of the triazole proton of (**4a**, *i.e.,* H^c) was similar to that of compound (**3**, *i.e.,* H^a), a smaller upfield shift of the aromatic proton (H^d) in compound (**4a**) was observed (0.01 ppm H^d). The addition of a further three equivalents of Ag(I) then resulted in a gradual return towards its original position (Fig. S7), a trend also observed for (**4b**) (Fig. S8). The calculated Ag(I)-binding constants[14] revealed the binding affinity of (**4b**) (752 ± 43 M^{-1}) was slightly higher than (**4a**, 533 ± 26 M^{-1}) and (**3**, 478 ± 32 M^{-1}). Taken collectively, the weaker Ag(I)-binding ligand (**3**) chelates Ag(I) *via* a similar mechanism to (**2**),[9a] whereas the bulkier ligands (**4a-b**) bind Ag(I) much akin to ligand (**1**).[9b] Colloidal stability studies in aqueous NaCl revealed aggregation of AgNP@(**3**) occurred at 0.5 M NaCl after 24 hours (Fig. S10). In contrast, aggregation of AgNP@(**4a**)/(**4b**) occurred at a higher NaCl concentration (1.0 M) but were stable in 0.5 M NaCl for 24 hours.

The interaction of each ligand with the AgNP surface was then explored using surface-enhanced Raman scattering (SERS, Fig. 3a). A strong band in the AgNP@(**3**) Raman spectrum at 1788 cm^{-1} is present in AgNP@(**3**), which is indicative of the presence of a C=O stretch (Fig. 3b).[15] The absence of such a stretch in the SERS spectra of AgNP@(**4a**) and AgNP@(**4b**) infers that the C1' carboxylate of the galactose sugars of AgNP@(**3**) are in close contact with the silver surface. The lack of a similar feature in the SERS spectra of AgNP@(**4a**) and AgNP@(**4b**) suggests that the carboxylate groups of (**4a-b**) adopt a conformation away from the AgNP surface.[16] Changes in the orientation of the ligand on the AgNP surface of AgNP@(**4a**) and AgNP@(**4b**) was also evident in other regions of the SERS spectra. For example, the SERS spectrum for AgNP@(**4a**) exhibited strong bands at 986 cm^{-1} (1,3,5 trisubstituted C-H deformation) and 1619 cm^{-1} (aromatic –C=C- stretch) indicative of close contact between the resorcinol core and the silver surface (Fig. 3a). In contrast, these bands were absent in AgNP@(**4b**). This could be due to the constrained nature of the ligand, with the placement of the EG tail much closer to the surface in AgNP@(**4a**) compared to AgNP@(**4b**). The SERS spectra of the free ligands (**3**, **4a-b**) show broadly similar spectra with the same major peaks at 996 cm^{-1} (1,3,5 trisubstituted C-H deformation) and 1026 cm^{-1} (C-C stretch + C-H deformation).[17]

Finally, the preparation of nanotagged variants of AgNP@(**3**, **4a-b**) was explored.[18,19] MGITC has been used previously as a sensitive SERS reporter that functions by directly interacting with the surface of AuNP *via* its isothiocyanate (ITC) group.[1d, 20] Indeed when MG was used, no SERS signal was observed in the diagnostic region 1150 - 1300 cm^{-1} at 100 nM concentration.

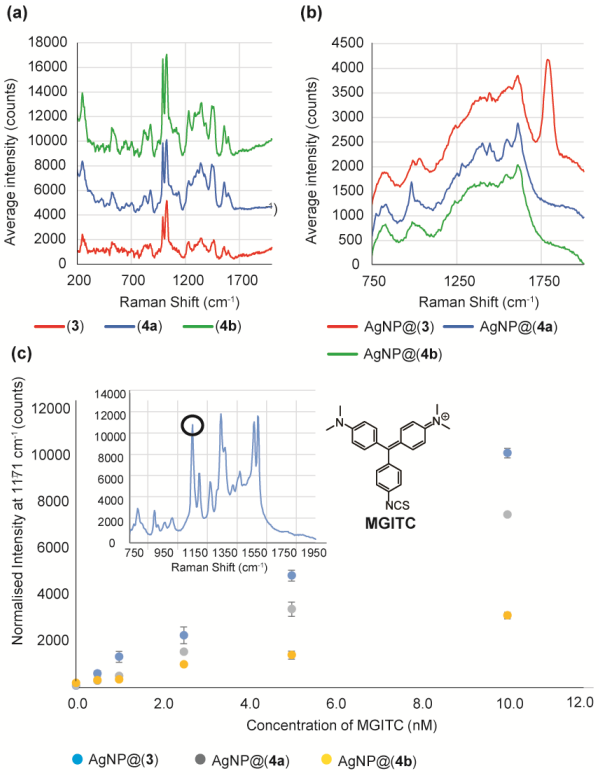

Fig. 3. (a) Stacked Raman spectra of sugar ligands (785 nm excitation; 1 accumulation; 1 s scan (**3**); 10 s scan (**4a**); 5 s scan (**4b**). **(b)** Stacked SERS spectra of AgNP@(**3**), AgNP@(**4a**) and AgNP@(**4b**) (532 nm excitation; 1 s scan; 1 accumulation). **(c)** Plot of the intensity of the 1171 cm^{-1} peak of MGITC using AgNP@(**3, 4a-b**) at decreasing concentrations of MGITC. Inset- SERS spectrum of MGITC using AgNP@(**4a**) highlighting the peak of interest.

In contrast, an intense signal for MGITC was observed for all three AgNP systems at this concentration (Fig. S11). Finally, the sensitivity limits of the MGITC group were explored with each AgNP type in more detail. Fig. 3c shows that all three AgNPs can reproducibly detect MGITC down to 0.5 nM. Since Raman enhancement is only observed using MGITC, we conclude that this is most likely due to a direct interaction between the ITC group of MGITC and the AgNP surface; much akin to previous observations using AuNPs.[20] We therefore conclude that the combined attributes of colloidal stability in aqueous buffers and selective SERS enhancement demonstrates the potential utility of these AgNP systems for their further development into a biosensing platforms.

In summary, we have described a facile, one-pot synthetic strategy to produce stable and monodisperse AgNP colloids using sugar triazole ligands. This work has identified the southernmost triazole as a modular site to tune the physical properties of AgNPs. Additionally, the installation of EG tails opens up new opportunities for further molecular elaboration, ranging from fine-tuning these systems for biosensing,[21] optical imaging[22] and broader nanotechnology[23] applications.

Acknowledgements

H. A. K. thanks the University of King Abdulaziz in Saudi Arabia for a postgraduate studentship. A. W. C. thanks the Royal Academy of Engineering (grant number 10216/103), the James Watt Nanofabrication Centre, and the Kelvin Nanocharacterisation Centre at the University of Glasgow. D. G. thanks the Royal Society for support through a Wolfson Merit Award.

References

1. (a) X. Lu, M. Rycenga, S. E. Skrabalak, B. Wiley and Y. Xia, *Ann. Rev. Phys. Chem.*, 2009, **60**, 167; (b) M. Rycenga, C. M. Cobley, J. Zeng, W. Li, C. H. Moran, Q. Zhang, D. Qin and Y. Xia, *Chem. Rev.*, 2011, **111**, 3669; (c) L. Guerrini and D. Graham, *Chem. Soc. Rev.*, 2012, **41**, 7085; (d) X. M. Qian, X. H. Peng, D. O. Ansari, Q. Yin-Goen, G. Z. Chen, D. M. Shin, L. Yang, A. N. Young, M. D. Wang and S. M. Nie, *Nature Biotechnology*, 2008, **26**, 83; (e) M. R. Langille, M. L. Personick and C. A. Mirkin, *Angew. Chemie-Int. Ed.*, 2013, **52**, 13910; (f) A. R. Tao, S. Habas and P. D. Yang, Small, 2008, 4, 310; fH. W. Liao, C. L. Nehl and J. H. Hafner, *Nanomedicine*, 2006, **1**, 201.

2. Y. N. Xia, X. H. Xia, Y. Wang and S. F. Xie, *MRS Bulletin*, 2013, **38**, 335.

3. (a) L. Mulfinger, S. D. Solomon, M. Bahadory, A. V. Jeyarajasingam, S. A. Rutkowsky and C. Boritz, *J. Chem. Ed.*, 2007, **84**, 322; (b) R. Desai, V. Mankad, S. K. Gupta and P. K. Jha, *Nanosci. Nanotech. Lett.*, 2012, **4**, 30.

4. N. G. Bastús, F. Merkoçi, J. Piella and V. Puntes, *Chem. Mat.*, 2014, **26**, 2836.

5. B. Wiley, T. Herricks, Y. Sun and Y. Xia, *Nano Lett.*, 2004, **4**, 1733.

6. Y. G. Sun, B. Mayers, T. Herricks and Y. N. Xia, *Nano Lett.*, 2003, **3**, 955.

7. B. Pietrobon and V. Kitaev, *Chem. Mat.*, 2008, **20**, 5186.

8. (a) Y. D. Yin, Z. Y. Li, Z. Y. Zhong, B. Gates, Y. N. Xia and S. Venkateswaran, *J. Mat. Chem.*, 2002, **12**, 522; (b) A. Panacek, R. Prucek, J. Hrbac, T. Nevecna, J. Steffkova, R. Zboril and L. Kvitek, *Chem. Mat.*, 2014, **26**, 1332; (c) J. Soukupova, L. Kvitek, A. Panacek, T. j. Nevecna and R. Zboril, *Mat. Chem. Phys.*, 2008, **111**, 77; (d) L. Kvitek, A. Panacek, J. Soukupova, M. Kolar, R. Vecerova, R. Prucek, M. Holecova and R. Zboril, *J. Phys. Chem. C*, 2008, 112, 5825; (e) A. Panacek, L. Kvitek, R. Prucek, M. Kolar, R. Vecerova, N. Pizurova, V. K. Sharma, T. j. Nevecna and R. Zboril, *J. Phys. Chem. B*, 2006, **110**, 16248; (f) L. Kvitek, R. Prucek, A. Panacek, R. Novotny, J. Hrbac and R. Zboril, *J. Mat. Chem.*, 2005, **15**, 1099.

9. (a) H. A. Kashmery, A. W. Clark, R. Dondi, A. J. Fallows, P. M. Cullis and G. A. Burley, *Eur. J. Inorg. Chem.*, 2014, **28**, 4886; (b) R. Dondi, W. Su, G. A. Griffith, G. Clark and G. A. Burley, *Small*, 2012, **8**, 770.

10. (a) J. C. Jewett and C. R. Bertozzi, *Chem. Soc. Rev.*, 2010, **39**, 1272; (b) M. F. Debets, S. S. Van Berkel, J. Dommerholt, A. J. Dirks, F. Rutjes and F. L. Van Delft, *Acc. Chem. Res.*, 2011, **44**, 805; (c) C. Besanceney-Webler, H. Jiang, T. Q. Zheng, L. Feng, D. S. del Amo, W. Wang, L. M. Klivansky, F. L. Marlow, Y. Liu and P. Wu, *Angew. Chemie-Int. Ed.*, 2011, **50**, 8051.

11. J. M. Harris and R. B. Chess, *Nature Rev. Drug Discov.*, 2003, **2**, 214.

12. K. K. Maiti, U. S. Dinish, C. Y. Fu, J. J. Lee, K. S. Soh, S. W. Yun, R. Bhuvaneswari, M. Olivo and Y. T. Chang, *Biosensors & Bioelectronics*, 2010, **26**, 398.

13. (a) M. L. Gower and J. D. Crowley, *Dalton Trans.*, 2010, **39**, 2371; (b) J. D. Crowley, P. H. Bandeen and L. R. Hanton, *Polyhedron*, 2010, **29**, 70.

14. M. J. Hynes, *J. Chem. Soc., Dalton Trans.*, 1993, 311-312.

15. G. Socrates, Infrared and Raman Characteristic Group Frequencies: Tables and Charts, Chichester ; New York : Wiley, 3rd edtiion edn., 2001.

16. (a) M. Moskovits and J. S. Suh, *J. Phys. Chem.*, 1984, **88**, 5526; (b) X. Gao, J. P. Davies and M. J. Weaver, *J. Phys. Chem.*, 1990, **94**, 6858.

17. A. A. Jbarah, A. Ihle, K. Banert and R. Holze, *J. Raman Spec.*, 2006, **37**, 123.

18. (a) T. Donnelly, W. E. Smith, K. Faulds and D. Graham, *Chemical Commun.*, 2014, **50**, 12907; (b) H. Zhang, M. H. Harpster, W. C. Wilson and P. A. Johnson, *Langmuir*, 2012, **28**, 4030.

19. (a) A. W. Clark, D. G. Thompson, D. Graham and J. M. Cooper, *Adv. Mat.*, 2014, **26**, 4286; (b) K. Sivashanmugan, J.-D. Liao, B. H. Liu, C.-K. Yao and S.-C. Luo, *Sensors and Actuators B: Chemical*, 2015, **207**, 430; (c) A. La Porta, M. Grzelczak and L. M. Liz-Marzán, *ChemistryOpen*, 2014, **3**, 146.

20 X. Qian, S. R. Emory and S. Nie, *J. Am. Chem. Soc.*, 2012, **134**, 2000.

21. (a) Y. Zhao, L. Xu, W. Ma, L. Wang, H. Kuang, C. Xu and N. A. Kotov, *Nano Lett.*, 2014, **14**, 3908; (b) J. M. Li, W. F. Ma, C. A. Wei, J. Guo, J. Hu and C. C. Wang, *J. Mat. Chem.*, 2011, **21**, 5992.

22. (a) W. Jiang, B. Y. S. Kim, J. T. Rutka and W. C. W. Chan, *Nature Nanotech.*, 2008, **3**, 145; (b) J. L. West and N. J. Halas, *Ann. Rev. Biomed. Eng.*, 2003, **5**, 285.

23. S. Pal, R. Varghese, Z. Deng, Z. Zhao, A. Kumar, H. Yan and Y. Liu, *Angew. Chemie-Int. Ed.*, 2011, **50**, 4176.

